

AD-A064 393

FORD AEROSPACE AND COMMUNICATIONS CORP NEWPORT BEACH --ETC F/G 20/6
MACHINE HOLOGRAPHY, PRELIMINARY REPORT.(U)
JAN 79

N00014-78-C-0659

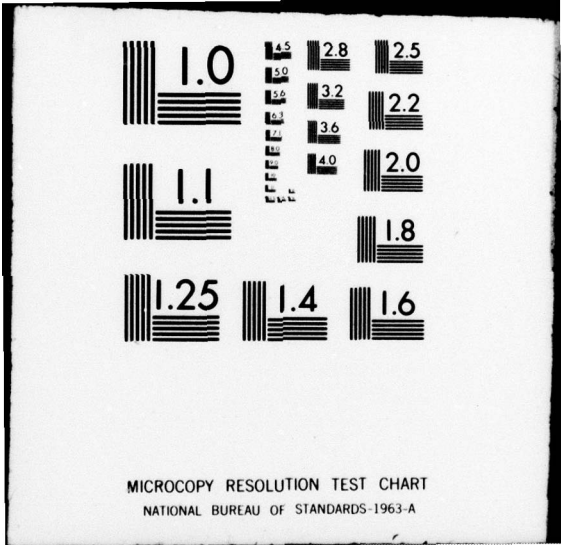
NL

UNCLASSIFIED

OF |
AD
A064393



END
DATE
FILMED
4 -79
DDC



MICROCOPY RESOLUTION TEST CHART
NATIONAL BUREAU OF STANDARDS-1963-A

LEVEL

12



Ford Aerospace & Communications Corporation

Aeronutronic Division

Ford Road
Newport Beach, California 92663
G081-78-2668

January 2, 1979

Department of the Navy
Office of Naval Research, Branch Office
1030 East Green Street
Pasadena, California 91106

Attention: Dr. E. T. Florance

Subject: Progress Report (CDRL A001) Aug. 1978^{new} Dec 78

Reference: Contract N00014-78-C-0659^{new}

Gentlemen:

In accordance with the Contract Data Requirements List (CDRL) Sequence Number A001 of the referenced contract, enclosed are two (2) copies of the subject report.

Should you have any questions regarding this submittal, please contact our Dr. C. Richards at (714) 759-6221.

Very truly yours,

Thomas P. Miller
Contract Administrator
Advanced Development Operation

TPM:lai

Enclosures

- cc: W. Luke, DCRL-GACA-43(1)
- NRL Director, Code 2627 (6)
- DDC (12)
- ONR, Dr. L. Haynes Code 437 (1)
- Captain R. L. Martin, USS Francis Marion (1)

ACCESSION BY	
DTIC	Staff Section <input checked="" type="checkbox"/>
DDC	Staff Section <input type="checkbox"/>
UNANNOUNCED	<input type="checkbox"/>
NOTIFICATION	
Per Hq. on file	
BY	DISTRIBUTION/AVAILABILITY CODES
DECL	AVAIL and/or SPECIAL
A	

ADA 064393

DDC FILE COPY

DDC
RECORDED
FEB 1 1979
D

DISTRIBUTION STATEMENT A
Approved for public release;
Distribution Unlimited

79 01 08 029

⑨ Progress Rept. Aug-Dec 78.

12

⑪ 2 Jan 79

⑥ MACHINE HOLOGRAPHY,
PRELIMINARY REPORT.

⑫ 70 p.

INTRODUCTION:

This report summarizes the principal results achieved so far in this contract. The primary tasks proposed were an examination of the information storage capacity of a conventional multiplexed hologram and also an effort to show that a hologram is capable of feature extraction. Both these tasks have been successfully accomplished. The latter effort led to a new concept with surprisingly great potential in pattern recognition and artificial intelligence.

⑮ N00014-78-C-0659

CONVENTIONAL MULTIPLEXED HOLOGRAMS:

In the first part of the contract, a theoretical and experimental investigation was made of the properties of a conventional multiplexed hologram. The experimental arrangement involved computer simulation of holograms and images arranged in a 64 x 64 pixel field-of-view. Connecting the image and hologram planes were discrete Fourier transforms. For this arrangement an equation was derived which gave the total amount of information which could be stored by conventional multiplexing. Here conventional multiplexing is defined to be the simple addition of subholograms to make the final multiplexed hologram. Thus:

$$H(\xi) = R_1^*(\xi) S_1(\xi) + R_2^*(\xi) S_2(\xi) + R_3^* S_3 + \dots \quad (1)$$

WHERE a single index ξ represents the two dimensions of the hologram in the Fourier plane.

Given this definition of multiplexing, the storage capacity of the hologram was predicted as:

$$D = ph = \frac{\eta}{\left(\frac{S}{N}\right)_A}^2 \quad (2)$$

- WHERE: D = total number of data pixels = total data stored
- p = number of reconstructed pixels in each subject scene, $s(x)$.
- h = number of subholograms in ensemble.
- η = number of pixels or degrees of freedom in hologram and image field.

394 853 79 01 08 029

slt

$$\left(\frac{S}{N}\right)_A = \text{reconstruction amplitude signal to noise ratio.}$$

Note that Equation (2) predicts that the amount of data which can be stored is independent of how the pie is divided. We can have few holograms with many data pixels each or many holograms each reconstructing a few data pixels. This flexibility appears to be a new result.

In order to test Equation (2) a parametric study was designed. The reference patterns were selected from an ensemble of statistically uncorrelated random patterns $(r;(x))$. The subject patterns, $(s_i(x))$, were simple data arrays of one, four and sixteen points which were shifted to different locations in the field-of-view so as to eliminate ambiguity in the reconstruction process. The result of the experimentation was full confirmation of Equation (2).

ADAPTIVE HOLOGRAMS:

The second technical effort of the contract was the successful attempt to show that a hologram can be trained to distinguish between two highly correlated images.

The nature of the problem is as follows: During the formation of a hologram, a reference image, $r(x)$ and a subject image $s(x)$ are Fourier transformed to provide the patterns $R(\xi)$ and $S(\xi)$. The reference is complex conjugated and multiplied by the subject to form the hologram trace.

$$H(\xi) = R^*(\xi) S(\xi) \quad (3)$$

Upon reconstruction, the reference $r(x)$ is reinserted, transformed and then modulated by the hologram. Immediately downstream of the hologram, the result is:

$$\text{Intermediate Output} = R(\xi) R^*(\xi) S(\xi) \quad (4)$$

This result is processed through an inverse Fourier transform and the final output image is:

$$I(x) = (r(x) \otimes r(x)) * s(x) \quad (5)$$

79² 01 08 029

Where $(r(x) \otimes r(x))$ is the autocorrelation of $s(x)$. This autocorrelation defines a point spread function for the reconstruction. The closer the point spread function is to a delta function, the better will be the quality of reconstruction.

Now suppose one reference $r_1(x)$ is used for the formation of a hologram using $s_1(x)$ as a subject while another, $r_2(x)$, is used for the reconstruction. The reconstructed image will then be:

$$I(x) = (r_1(x) \otimes r_2(x)) * s_1(x) \quad (6)$$

As long as r_1 is partially correlated with r_2 there will be a reconstruction of $s_1(x)$, although the amplitude of reconstruction will be reduced as the correlation coefficient declines. This property is useful for pattern recognition because with it, similar reference images, (r_1) , can produce the same output.

However, suppose we wish to form the hologram in such a way that the second reference, r_2 , produces a completely different output, s_2 , with no trace of s_1 showing. Can this be done? The proposed answer was "yes." The method suggested was to form a multiplexed hologram such that the correlated portions of r_1 and r_2 cancelled out, leaving the uncorrelated, or orthogonal parts, as features which can independently reconstruct two separate subject images s_1 and s_2 . This technique recognizes that residual crosstalk remains in the form of a random background of noise distributed over the field-of-view. The rules governing this crosstalk are the same as led to the derivation of Equation (2).

During the development of an algorithm to accomplish this cancellation task it was realized that the addition of a negative feedback loop around the hologram would automate the process. The result is a linear circuit of the form illustrated in Figure (1). In this circuit the hologram records the function $A(\xi)$ which is delivered by the summing junction. This recording is weighted by a convergence constant, c , and added to the pre-existing stock of the multiplexed hologram. Given reasonable care the process can be made to converge so that the hologram takes on a limit value. In effect the hologram acts as an adaptive servo controller and the object being servo controlled is the hologram itself:

This response of the system can be described by the first order differential equation (in the spatial Fourier plane):

$$\frac{dH(\xi, t)}{dt} + c |R(\xi)|^2 H(\xi, t) = c R^*(\xi) S(\xi) \quad (7)$$

WHERE R and S are coincident time dependent step function inputs.

The time response of the system is then;

$$H(\xi, t) = \frac{S(\xi)}{R(\xi)} (1 - \exp(-c |R(\xi)|^2 t)) \quad (8)$$

There are several points of significance here. First, although the hologram starts out having the form $H = R^*S$, it ultimately converges to the form $H = S/R$.

If we write this end result as;

$$H = \frac{S(\xi)}{R(\xi)} = \left(\frac{R^*(\xi)}{R(\xi) R^*(\xi)} \right) S(\xi) \quad (9)$$

We note that the coefficient function of $S(\xi)$ becomes just the ideal Wiener matched filter for the reference $r(x)$. Thus, adding a feedback loop and causing the hologram to adapt results in the hologram adapting to become an optimum filter.

The second point is that the time constant for the process:

$$\tau(\xi) = \frac{1}{c |R(\xi)|^2} \quad (10)$$

is a function of the power spectral density. High magnitude spectral components adapt (exponentially) much faster than low magnitude values. A corollary of Equation (10) is that where the amplitude $R(\xi) = 0$, the time constant will be infinite and no adaptation takes place. This leads to the third important point. Normally, $S(\xi)/R(\xi)$ will have infinities where $R(\xi)$ is zero. But this adaptive system takes infinitely long to adapt at these points so the infinities never develop. The system thus remains physically realizable.

A number of experiments were performed to demonstrate the power of the device, one of which is illustrated in Figure (2). Here, the image of a square is used as the reference or image to be recognized. It is tasked to

reconstruct the subject which is an image of a W. Because the autocorrelation of the reference is not entirely delta function like, the reconstructed image is initially broadened. In conventional holography this would be the best result that could be obtained. With the adaptive system, however, a few iterations serve to suppress the errors produced by the point spread function and the reconstructed image cleans up.

Having verified the basic properties described by Equations (7) and (8), attention was turned to the proposed requirement of having two similar reference patterns reconstruct two entirely different subject patterns with limited, or no, crosstalk. The results of this experiment are illustrated in Figure (3).

The references chosen were a normal square and a narrowed square. The narrow square was paired with a subject which was the image of the letter, N. The normal or wide square was paired with the letter W. The training process was very simple. The narrow square and N were presented to the system and the system adapted in its usual fashion. Then the wide square and W were presented and the system adapted to the new inputs. This simple alternate presentation process was repeated until the system equilibrated and the training was then completed.

At the beginning of the process there was considerable crosstalk with the wide square reconstructing the N image as well as the W and vice versa. (Note that the W and N are located in different places in the FOV so that any false reconstructions would be obvious.) After full equilibrium is reached all of the false reconstructions and crosstalk are eliminated so that the two reference images, played through the adaptively multiplexed hologram, reconstruct only the desired subjects. The technique appears to successfully perform a feature extraction and virtual orthogonalization of the two similar reference images. The illustration of the experiment in Figure (3) shows an adaptation which has not gone completely to equilibrium. Further experiments have shown that almost all the remaining crosstalk gets cleaned up.

The implications of this adaptive system are quite significant. One of the most important appears to be that the adaptive hologram seems to be capable of storing vastly more information than can the conventional multiplexed hologram. It seems likely (though untested) that Equation (2) no longer holds for the adaptive hologram.

Instead the correct equation is probably:

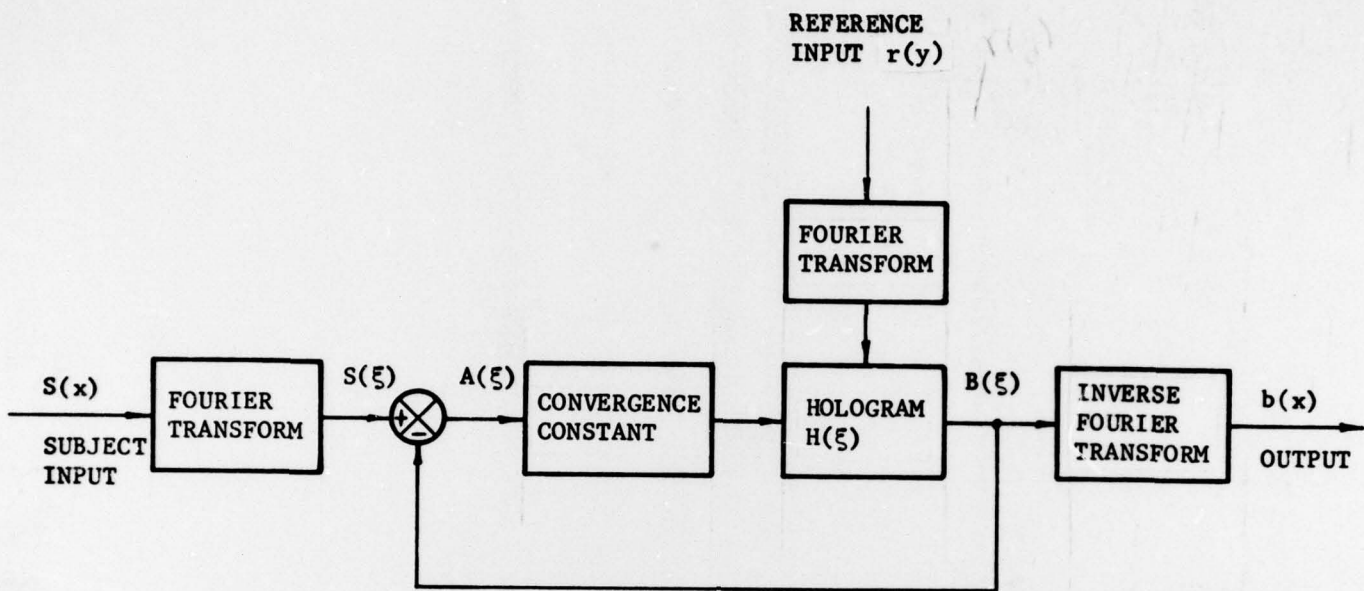
$$D = n^2 \quad (11)$$

With arbitrarily large reconstruction signal to noise ratio.

The reasoning behind this is that with the crosstalk eliminated, the system is capable of storing as many image vectors as there are linearly, independent basis vectors (that is to say n images). Furthermore, each image vector is composed of up to n basis vectors or pixels, for either the reference or the subject. Thus, each pixel gets used up to n times.

CONCLUSION:

The discovery, during this contract of the adaptive hologram opens up broad areas for theoretical and experimental investigation. Applications range from pattern recognition and artificial intelligence to investigations of the properties of the nervous system.



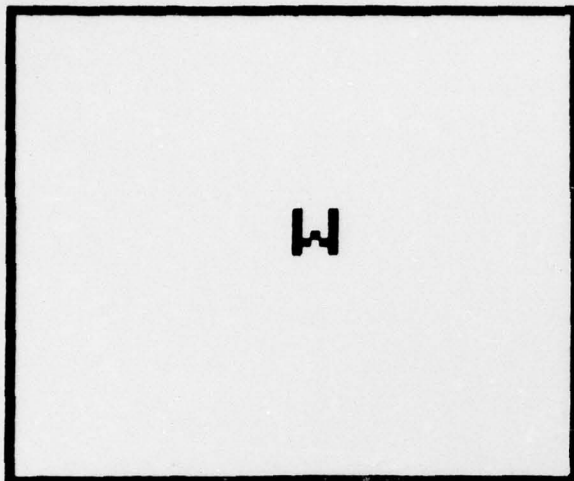
SYSTEM RESPONSE DIFFERENTIAL EQUATION:

$$(1) \quad \frac{dH(\xi, t)}{dt} + c |R(\xi)|^2 H(\xi, t) = cR^*(\xi) S(\xi)$$

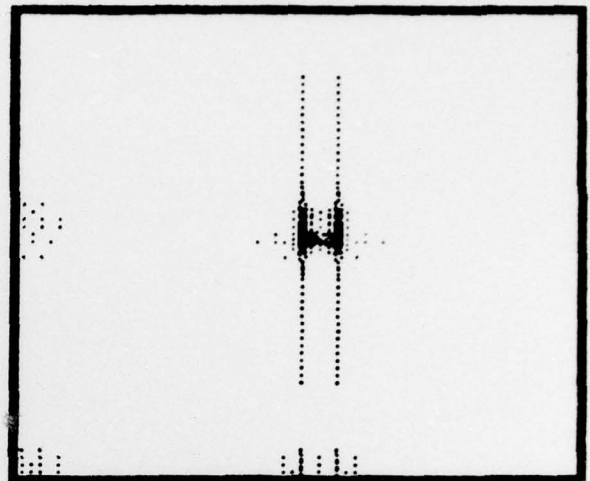
TIME RESPONSE EQUATION:

$$(2) \quad H(\xi, t) = \frac{S(\xi)}{R(\xi)} (1 - \exp[-c |R(\xi)|^2 t])$$

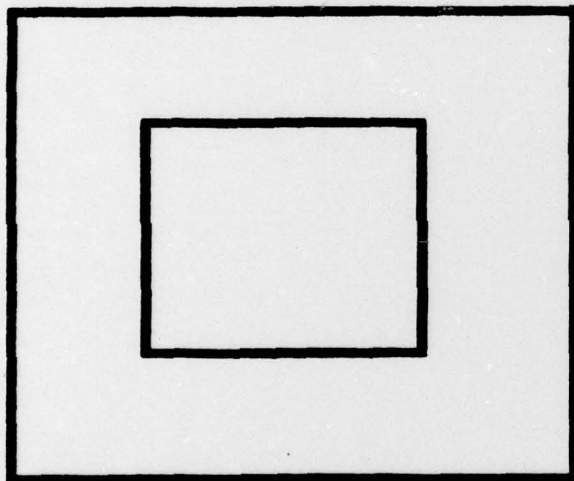
FIGURE 1. ADAPTIVE HOLOGRAPHIC SYSTEM WITH FEEDBACK LOOP INSIDE FOURIER TRANSFORMS



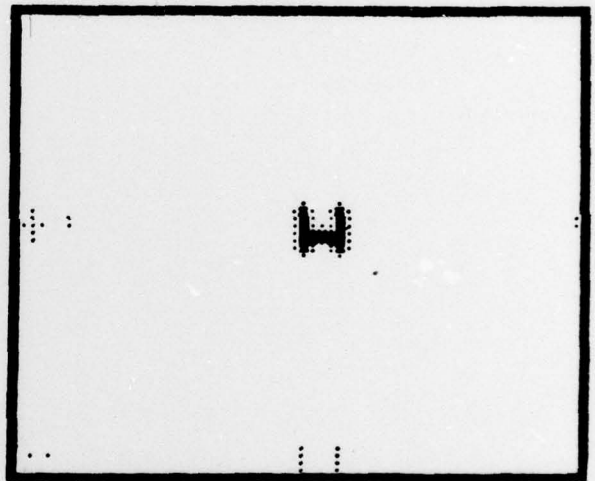
SUBJECT



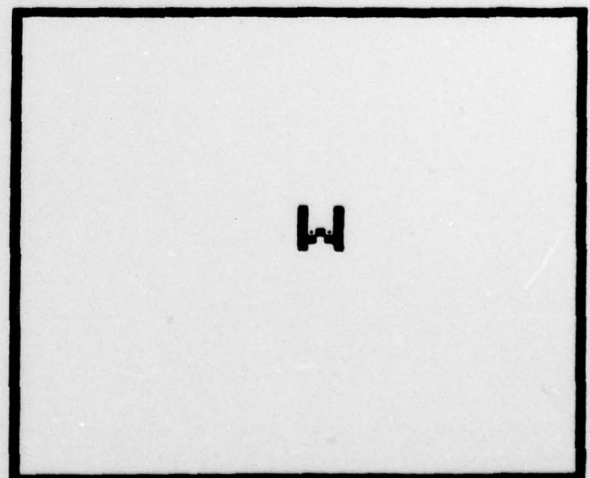
INITIAL RECONSTRUCTION OF SUBJECT



REFERENCE
(PATTERN TO BE RECOGNIZED)

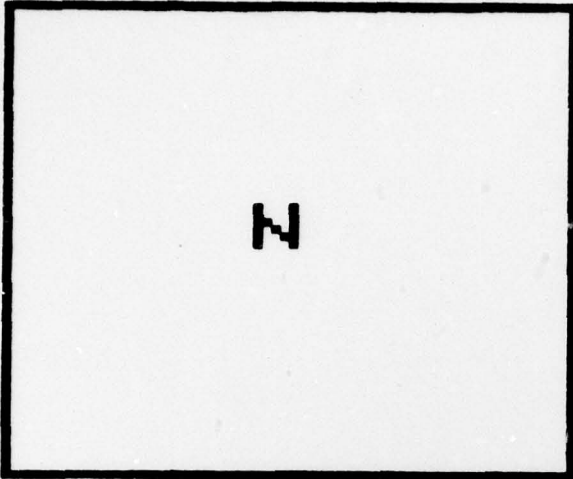


RECONSTRUCTION AFTER ITERATION



RECONSTRUCTION WITH ITERATION
PROCESS NEARING COMPLETION

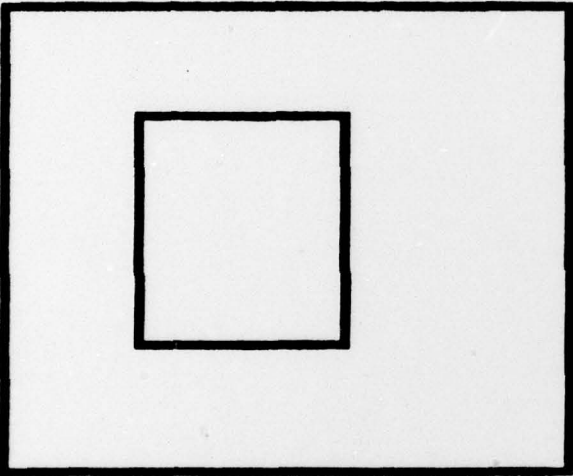
FIGURE 2. EXAMPLE OF ELIMINATION OF RECONSTRUCTION ERRORS BY USING AN ADAPTIVE HOLOGRAM WITH NEGATIVE FEEDBACK. THE FEEDBACK LOOP IS INSIDE THE TRANSFORMS.



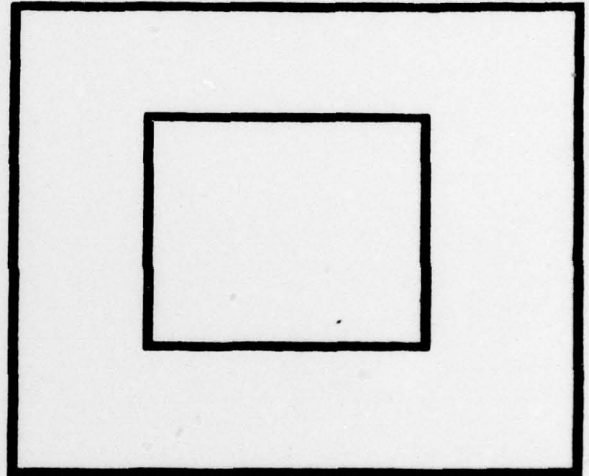
SUBJECT 1



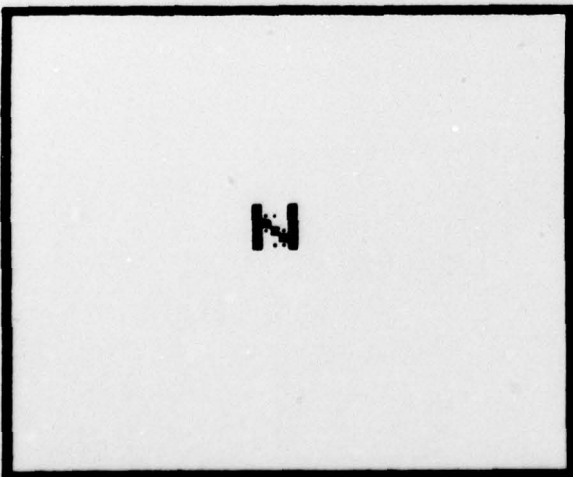
SUBJECT 2



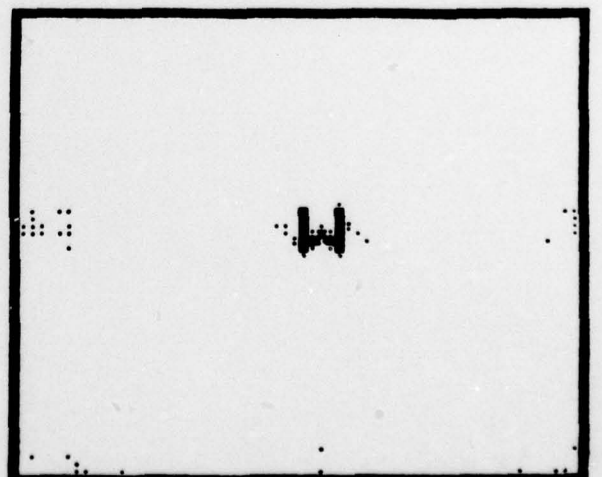
REFERENCE 1



REFERENCE 2



RECONSTRUCTION WITH REFERENCE 1



RECONSTRUCTION WITH REFERENCE 2

FIGURE 3. EXAMPLE OF SYSTEM TRAINED TO DISTINGUISH BETWEEN TWO SIMILAR PATTERNS